

Microscopic study of collective excitations in rotating nuclei

J. Kvasil,¹ N. Lo Iudice,² R. G. Nazmitdinov,^{3,4} A. Porrino,² and F. Knapp¹

¹*Institute of Particle and Nuclear Physics,
Charles University, V.Holešovičkách 2,
CZ-18000 Praha 8, Czech Republic*

²*Dipartimento di Scienze Fisiche, Università di Napoli "Federico II"
and Istituto Nazionale di Fisica Nucleare,
Monte S Angelo, Via Cinthia I-80126 Napoli, Italy*

³*Departament de Física, Universitat de les Illes Balears,
E-07122 Palma de Mallorca, Spain*

⁴*Bogoliubov Laboratory of Theoretical Physics,
Joint Institute for Nuclear Research, 141980 Dubna, Russia*

(Dated: November 8, 2018)

Abstract

We have carried out a unified microscopic study of electric monopole, quadrupole and magnetic dipole excitations in fast rotating nuclei undergoing backbending, with special attention at the magnetic excitations. We found, among other results, that the strength of the orbital magnetic dipole excitations (scissors mode) gets enhanced by more than a factor four at high rotational frequency, above the backbending region. We provide a physical explanation for such an enhancement.

PACS numbers: 21.10.Re,21.60.Jz,27.70.+q

I. INTRODUCTION

Deformation is known to affect deeply the collective nuclear motion [1]. We mention here the split of the electric giant dipole (E1) [2, 3], quadrupole (E2) [4] and octupole (E3) [5, 6] resonances, as well as the coupling between quadrupole and monopole (E0) modes [7, 8, 9]. It generates also a completely new excitation, the scissors mode [10, 11, 12].

With the advent of heavy-ion accelerators and of a new generation of detectors, it was possible to get access to fast rotating nuclei and to observe quite new phenomena induced by the rapid rotation. Backbending is a well known spectacular example [13]. Systematic theoretical investigations have clarified to a great extent how fast rotation affects most of the nuclear properties, including $\beta-$ and $\gamma-$ modes [14, 15], low-lying octupole excitations and alignment [16, 17, 18], pairing vibrations [19, 20]. All these studies were carried out in cranked random-phase-approximation (CRPA) using separable effective interactions. The same approach was adopted for extensive studies of the E1 giant resonance [21, 22].

Less explored is the effect of rotation on other collective excitations. To our knowledge, monopole and quadrupole resonances were studied only in [23] within the CRPA, using the cranked modified harmonic oscillator (HO), and in [9] within a phonon plus rotor model, using schematic RPA to generate the phonons.

In the present paper, we intend to complete the analysis of Refs. [9, 23] by including the study of the magnetic dipole (M1) excitations, specially the orbital ones known as scissors mode. This, in fact, not only is intimately linked to deformation and, more in general, to quadrupole correlations, but, by its own nature, is also strictly correlated with nuclear rotation. Its properties might therefore change considerably in going from slow to fast rotating nuclei.

Our procedure is framed within the CRPA and parallels closely the model of Ref. [18]. We adopted, in fact, a cranked Nilsson model plus quasiparticle RPA and made use of doubly stretched coordinates. There are, on the other hand, several differences concerning mainly the choice and treatment of the Hamiltonian as well as the method of computing the electromagnetic response.

We applied our method to ^{156}Dy and ^{158}Er . The evolution of their moment of inertia with the rotational frequency was studied within an approach using the same mean field adopted here and found to be consistent with the behavior observed experimentally, including the

backbending region [24]. This strengthens our confidence on the reliability of our predictions on the M1 mode, whose properties, as we shall see, depend critically on the nuclear moment of inertia.

II. RPA IN THE ROTATING FRAME

A. The Hamiltonian

We started with the Hamiltonian

$$H_\Omega = H - \hbar\Omega\hat{I}_1 = H_0 - \sum_{\tau=n,p} \lambda_\tau N_\tau - \hbar\Omega I_1 + V. \quad (1)$$

The unperturbed piece is composed of two terms

$$H_0 = \sum_i (h_{Nil}(i) + h_{add}(i)). \quad (2)$$

The first is the Nilsson Hamiltonian

$$h_{Nil} = \frac{p^2}{2m} + V_{HO} + v_{ls}\mathbf{l} \cdot \mathbf{s} + v_{ll}(\mathbf{l}^2 - \langle \mathbf{l}^2 \rangle_N), \quad (3)$$

where

$$V_{HO} = \frac{1}{2}m(\omega_1^2 x_1^2 + \omega_2^2 x_2^2 + \omega_3^2 x_3^2) \quad (4)$$

is a triaxial HO, whose frequencies satisfy the volume conserving condition $\omega_1\omega_2\omega_3 = \omega_0^3$. The second comes from restoring the local Galilean invariance broken in the rotating coordinate systems and has the form [18]

$$h_{add} = -\frac{\Omega}{\sqrt{\omega_2\omega_3}} \left\{ v_{ll} \left[2m\omega_0 \mathbf{r}'^2 - \hbar \left(N_{(osc)} + \frac{3}{2} \right) \right] l'_1 + v_{ls}m\omega_0 [\mathbf{r}'^2 \mathbf{s}_1 - \mathbf{x}'_1(\mathbf{r}' \cdot \mathbf{s})] \right\}, \quad (5)$$

where $x'_i = (\omega_i/\omega_0)^{1/2}x_i$ are single-stretched coordinates.

The two-body potential has the following structure

$$V = V_{PP} + V_{QQ} + V_{MM} + W_{\sigma\sigma}. \quad (6)$$

V_{PP} is a monopole pairing interaction

$$V_{PP} = - \sum_{\tau=p,n} G_\tau P_\tau^\dagger P_\tau, \quad (7)$$

where $P_\tau^\dagger = \sum_k a_k^\dagger a_{\bar{k}}^\dagger$ is the usual pairing operator. V_{QQ} and V_{MM} are, respectively, separable quadrupole-quadrupole and monopole-monopole interactions

$$\begin{aligned} V_{QQ} &= -\frac{1}{2} \sum_{T=0,1} \kappa(T) \sum_{r=\pm} \sum_{\mu=0,1,2} (\tilde{Q}_\mu [{}_r^T])^2, \\ V_{MM} &= -\frac{1}{2} \sum_{T=0,1} \kappa(T) (\tilde{M} [{}_{r=+}^T])^2. \end{aligned} \quad (8)$$

$V_{\sigma\sigma}$ is a spin-spin interaction

$$V_{\sigma\sigma} = -\frac{1}{2} \sum_{T=0,1} \kappa_\sigma(T) \sum_{r=\pm} \sum_{\mu=0,1} (s_\mu [{}_r^T])^2. \quad (9)$$

Because of its repulsive character, this interaction pushes the spin excitations at higher energy, thereby generating two well separated regions, one below 4 MeV, composed of mainly orbital excitations and another, in the range 4 MeV \div 12 MeV, characterized by spin excitations [25, 26].

All the one-body fields have good isospin T and signature r . Multipole and spin-multipole fields of good signature are defined in Ref. [27]. The tilde indicates that monopole and quadrupole fields are expressed in terms of doubly stretched coordinates $x_i'' = (\omega_i/\omega_0) x_i$ [4, 28]. In this new form, for a pure HO Hamiltonian, the quadrupole fields fulfill the stability conditions

$$\langle \tilde{Q}_\mu \rangle = 0, \quad \mu = 0, 1, 2 \quad (10)$$

if nuclear self-consistency

$$\omega_1^2 \langle x_1^2 \rangle = \omega_2^2 \langle x_2^2 \rangle = \omega_3^2 \langle x_3^2 \rangle \quad (11)$$

is satisfied in addition to the volume conserving condition. In virtue of the constraints (10), the interaction will not distort further the deformed HO potential, if the latter is generated as a Hartree field. This is achieved by starting with an isotropic HO potential of frequency ω_0 and, then, by generating the deformed part of the potential from the (unstretched) quadrupole-quadrupole interaction. The outcome of this procedure is

$$V_{HO} = \frac{m\omega_0^2 r^2}{2} - m\omega_0^2 \beta \cos\gamma Q_0 [{}_+^0] - m\omega_0^2 \beta \sin\gamma Q_2 [{}_+^0] \quad (12)$$

where

$$\begin{aligned} m\omega_0^2 \beta \cos\gamma &= \kappa[0] \langle Q_0 [{}_+^0] \rangle \\ m\omega_0^2 \beta \sin\gamma &= \kappa[0] \langle Q_2 [{}_+^0] \rangle \end{aligned} \quad (13)$$

The triaxial form given by Eq. (4) follows from defining

$$\omega_i = \omega_0 \exp\left[-\frac{2}{3}\delta \cos\left(\gamma - i\frac{2\pi}{3}\right)\right], \quad i = 1, 2, 3, \quad (14)$$

where the new deformation parameter is defined by $\beta = \sqrt{16\pi/45} \delta$. The Hartree conditions have the form given by Eq.(13) only for an HO plus a separable quadrupole-quadrupole potential. They change once pairing is included [29]. Moreover, they fail to give the minimum of the mean field energy of the rotating system in superdeformed nuclei [30]. For all these reasons, we have allowed for small deviations from Eqs. (13) and enforced, instead, the stability conditions (10). These, in fact, hold also in the presence of pairing [24] and guarantee the separation of the pure rotation from the intrinsic vibrational modes in the limit of rotating harmonic oscillator [31].

B. Quasiparticle RPA in rotating systems

We expressed first the Hamiltonian in terms of quasiparticle creation (α_i^\dagger) and annihilation (α_i) operators by carrying out at each rotational frequency Ω a generalized Bogoliubov transformation. We then faced the RPA problem and wrote the RPA equations in the form [14, 27]

$$[H_\Omega, P_\nu] = i\hbar\omega_\nu^2 X_\nu, \quad [H_\Omega, X_\nu] = -i\hbar P_\nu, \quad [X_\nu, P_{\nu'}] = i\hbar\delta_{\nu\nu'}, \quad (15)$$

where X_ν , P_ν are, respectively, the collective coordinates and their conjugate momenta. The solution of the above equations yields the RPA eigenvalues $\hbar\omega_\nu$ and eigenfunctions

$$\begin{aligned} |\nu\rangle = O_\nu^\dagger |RPA\rangle &= \frac{1}{\sqrt{2}} \left(\sqrt{\frac{\omega_\nu}{\hbar}} X_\nu - \frac{i}{\sqrt{\hbar\omega_\nu}} \hat{P}_\nu \right) |RPA\rangle \\ &= \sum_{ij} (\psi_{ij}^\nu b_{ij}^\dagger - \Phi_{ij}^\nu b_{ij}) |RPA\rangle, \end{aligned} \quad (16)$$

where $b_{ij}^\dagger = \alpha_i^\dagger \alpha_j^\dagger$ ($b_{ij} = \alpha_i \alpha_j$) creates (destroys) a pair of quasiparticles out of the RPA vacuum $|RPA\rangle$. Since the Hamiltonian can be decomposed into the sum of a positive and a negative signature piece

$$H_\Omega = H_\Omega(r=+) + H_\Omega(r=-), \quad (17)$$

we solved the eigenvalue equations (15) for $H_\Omega(+)$ and $H_\Omega(-)$ separately.

The symmetry properties of the cranking Hamiltonian yield

$$[H, N_{\tau=n,p}]_{RPA} = 0, \quad [H, I_1]_{RPA} = 0 \quad (18)$$

$$[H, I_2]_{RPA} = i\hbar\Omega I_3, \quad [H, I_3]_{RPA} = -i\hbar\Omega I_2. \quad (19)$$

The last two equations can be combined so as to obtain

$$[H_\Omega(-), \Gamma^\dagger] = \Omega\Gamma^\dagger \quad (20)$$

where $\Gamma^\dagger = (I_2 + iI_3)/\sqrt{2\langle I_1 \rangle}$ and $\Gamma = (\Gamma^\dagger)^\dagger = (I_2 - iI_3)/\sqrt{2\langle I_1 \rangle}$ fulfill the commutation relation

$$[\Gamma, \Gamma^\dagger] = 1. \quad (21)$$

According to Eqs. (18), we have two Goldstone modes, one associated to the violation of the particle number operator, the other is a positive signature zero frequency rotational solution associate to the breaking of spherical symmetry. Eq. (20), on the other hand, yields a negative signature redundant solution of energy $\omega_\lambda = \Omega$, which describes a collective rotational mode arising from the symmetries broken by the external rotational field (the cranking term).

Eqs. (18) and (20) guarantee the separation of the spurious or redundant solutions from the intrinsic ones. They would be automatically satisfied if the single-particle basis were generated through a self-consistent Hartree-Bogoliubov (HB) calculation. As we shall show, they are fulfilled with good accuracy also in our, not fully self-consistent, HB treatment.

The strength function for an electric ($X = E$) or magnetic ($X = M$) transition of multipolarity λ from a state of the yrast line with angular momentum I is

$$S_{X\lambda}(E) = \sum_{\nu I'} B(X\lambda, I \rightarrow I', \nu) \delta(E - \hbar\omega_\nu), \quad (22)$$

where ν labels all the excited states with a given I' . In order to compute the reduced strength $B(X\lambda, I \rightarrow I', \nu)$ we should be able to expand the intrinsic RPA state into components with good K quantum numbers, which is practically impossible in the cranking approach. We have, therefore, computed the strength in the limits of zero and high frequencies. For non rotating axially symmetric nuclei, whose initial state is usually the $I = 0, K^\pi = 0_{gr}^+$ ground state, the strength function is given by

$$S_{X\lambda}(E) = \sum_{\nu K} B(X\lambda, 0_{gr}^+ \rightarrow K\nu) \delta(E - \hbar\omega_\nu), \quad (23)$$

where

$$B(X\lambda, 0_{gr}^+ \rightarrow K_\nu) = | \langle RPA | [O_{K\nu}, \mathcal{M}(X\lambda\mu_3 = K)] | RPA \rangle |^2. \quad (24)$$

For fast rotating nuclei, we assumed a complete alignment of the angular momentum along the rotational x_1 -axis, so that ($I' = I + \Delta I$)

$$S_{X\lambda, \Omega(I)}(E) = \sum_{\nu \Delta I} B(X\lambda, I \text{ yrast} \rightarrow I + \Delta I, \nu r) \delta(E - \hbar\omega_\nu) \quad (25)$$

where ($\Delta I = 0, \pm 1, \dots, \pm \lambda$)

$$\begin{aligned} B(X\lambda, I \rightarrow I + \Delta I, \nu r) &= \\ &= | \langle II\lambda\Delta I | I + \Delta II + \Delta I \rangle_\Omega \langle RPA | [O_{\nu r}, \mathcal{M}(X\lambda\mu_1 = \Delta I)] | RPA \rangle_\Omega |^2, \end{aligned} \quad (26)$$

having denoted by $|RPA\rangle_\Omega$ the RPA vacuum (yrast state) at the rotational frequency Ω . The multipole operator in the rotating frame was obtained from the corresponding one in the laboratory according to the prescription [32]

$$\mathcal{M}(X\lambda\mu_1) = \sum_{\mu_3} \mathcal{D}_{\mu_1\mu_3}^\lambda(0, \frac{\pi}{2}, 0) \mathcal{M}(X\lambda\mu_3). \quad (27)$$

Having used an interaction composed of a sum of separable pieces, we did not need to determine explicitly the RPA eigenvalues and eigenfunctions in order to calculate the strength function. Following the method of Ref. [14, 27], we had just to replace the δ distribution with a Lorentz weight and, upon the use of the Cauchy theorem, we obtained for $S_{X\lambda}(E)$ and $S_{X\lambda, \Omega(I)}(E)$ expressions involving only two-quasiparticle matrix elements of one-body multipole operators.

The n -th moments were obtained simply as

$$m_n(X\lambda) = \int_0^\infty E^n S_{X\lambda}(E) dE. \quad (28)$$

The $m_0(X\lambda)$ and $m_1(X\lambda)$ moments give, respectively, the energy unweighted and weighted summed strengths.

III. NUMERICAL CALCULATIONS AND RESULTS

A. Determination of the parameters

We took the parameters of the rotating Nilsson potential from Ref. [33]. They were determined from a systematic analysis of the experimental single-particle levels of deformed

nuclei of rare earth and actinide regions. We included all shells up to $N = 8$ and accounted for the $\Delta N = 2$ mixing.

In principle, the pairing gap should have been determined self-consistently at each rotational frequency. In order to avoid unwanted singularities for certain values of Ω , we followed the phenomenological prescription [34]

$$\Delta_\tau(\Omega) = \begin{cases} \Delta_\tau(0) [1 - \frac{1}{2}(\frac{\Omega}{\Omega_c})^2] & \Omega < \Omega_c \\ \Delta_\tau(0) \frac{1}{2}(\frac{\Omega_c}{\Omega})^2 & \Omega > \Omega_c \end{cases}, \quad (29)$$

where Ω_c is the critical rotational frequency of the first band crossing. We got, for both neutrons and protons, $\Omega_c = 0.32$ MeV for ^{156}Dy and $\Omega_c = 0.33$ MeV for ^{158}Er . We extracted the values of the pairing gaps at zero rotational frequency from the odd-even mass difference obtaining $\Delta_N(0) = 0.857$ MeV, $\Delta_P(0) = 0.879$ MeV for ^{156}Dy and $\Delta_N(0) = 0.874$ MeV, $\Delta_P(0) = 0.884$ MeV for ^{158}Er . We used as input for our HB calculations the deformation

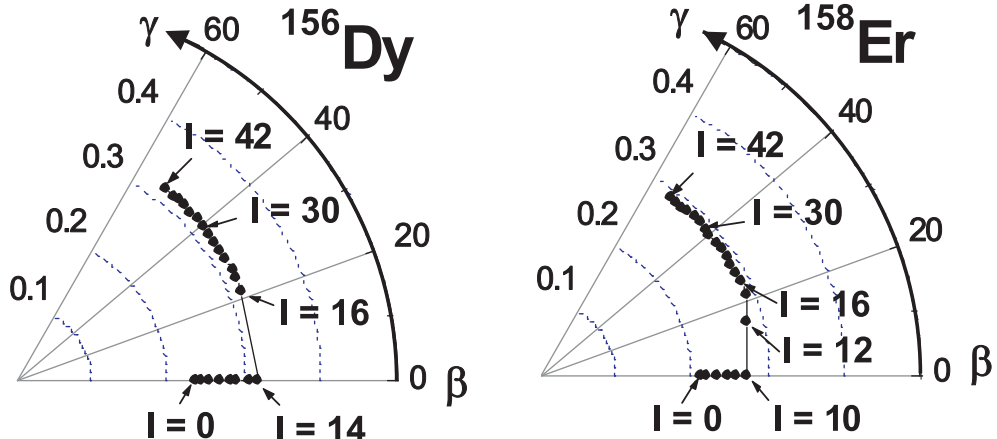


FIG. 1: (Color online) Yrast line deformations in β - γ plane as a function of the angular momentum.

parameters obtained from the empirical moments of inertia at each Ω [35]. As shown in Fig.1 and discussed elsewhere [24], triaxiality sets in at the frequency which triggers backbending as result of the vanishing of the gamma excitations of positive signature in the rotating frame.

The parameters so determined yield results in better agreement with experiments compared to the predictions of Ref. [36] for $N \sim 90$, where a fixed phenomenological inertial parameter was used for all Ω . Moreover, our equilibrium deformations are short from being the self-consistent solutions of the HB equations. Indeed, any deviation from the equilibrium values of the deformation parameters β and γ resulted into a higher HB energy. Dealing with

transitional nuclei, however, the minimum becomes very shallow as the rotational frequency increases. In fact, the energy minima for the collective rotations around the x_1 rotational axis and for the non collective ones around the x_3 symmetry axis are almost degenerate near the crossing point of the ground with the gamma band. The energy difference is about 15 keV near the critical rotational frequency where the backbending occurs. At the bifurcation point, the competition between the collective and non-collective rotations breaks the axial symmetry and yields non axial shapes. On the other hand, the doubly stretched quadrupole moments are approximately zero for all values of the equilibrium deformation parameters, consistently with the stability conditions (10). A small deviation from the equilibrium deformation yields a strong deviation of these moments from zero. We infer from the just discussed tests that our solutions are close to the self-consistent HB ones.

As for the strength κ of the monopole and quadrupole interactions, we started with adopting the standard HO formulas ($\lambda = 2$) [28]

$$\kappa_\lambda[0] = \frac{4\pi}{2\lambda+1} \frac{m\omega_0^2}{A \langle r^{2\lambda-2} \rangle}, \quad \kappa_\lambda[1] = -\frac{\pi V_1}{A \langle r^{2\lambda} \rangle}. \quad (30)$$

The isoscalar strength, for instance, follows from enforcing the Hartree self-consistent conditions. We then changed slightly the strengths at each rotational frequency, while keeping constant the $\kappa[1]/\kappa[0]$ ratio, so as to fulfill the RPA equations (18)-(20) for the spurious or redundant modes. The constants so determined differ from the HO ones by 5-10% at most. For the spin, we used the generally accepted strengths [37]

$$\kappa_\sigma[0] = \kappa_\sigma[1] = -28 \frac{4\pi}{A} MeV$$

for all rotational frequencies. Finally, we used bare charges to compute the $E0$ and $E2$ strengths and a quenching factor $g_s = 0.7$ for the gyromagnetic ratios to compute the $M1$ strengths.

With the above parameters, it was possible not only to separate the spurious and rotational solutions from the intrinsic modes, but also to reproduce the experimental dependence of the lowest β and γ bands on Ω and, in particular, to observe the crossing of the γ with the ground band in correspondence of the onset of triaxiality [24].

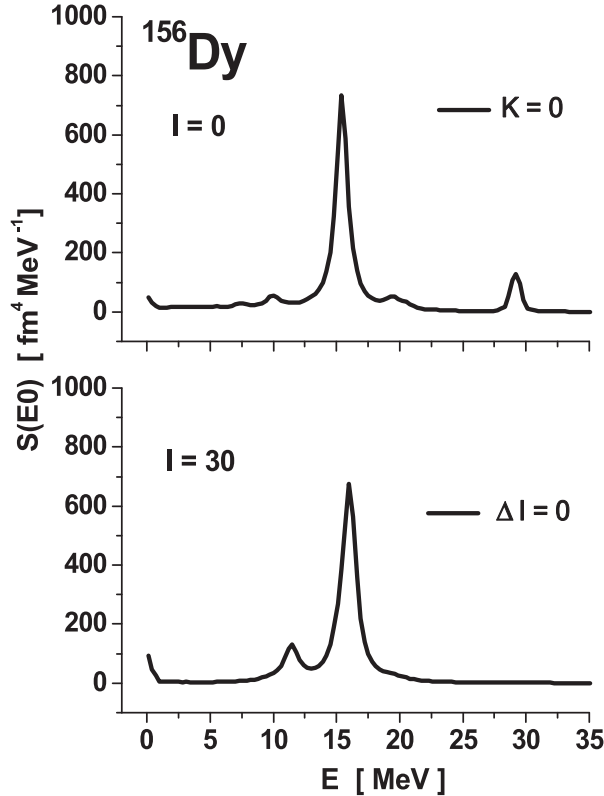


FIG. 2: E0 strength function at zero and high rotational frequencies in ^{156}Dy .

B. Evolution of transition strengths with rotation

We show only the results of ^{156}Dy , since the ones concerning ^{158}Er are very similar. As shown in Fig. 2, the $E0$ response remains unchanged in its dominant isoscalar peak. The effects of fast rotation get manifested through the suppression of the high energy isovector peak, small in any case, and the appearance of a peak at $\sim 11 \div 12$ MeV, in correspondence of the $K = 0$ branch of the quadrupole resonance. This result indicates that the coupling between monopole and $K = 0$ quadrupole modes gets stronger with increasing rotational frequency. Indeed, as triaxiality sets in at high frequencies, anisotropy increases, thereby enhancing the mixing between the two channels.

Rotation has some appreciable effects on the quadrupole transitions. It broadens considerably the isoscalar quadrupole giant resonance because of the increasing splitting of the different ΔI peaks with increasing Ω . It washes out the isovector $E2$ resonance for the same reason. The low-lying peaks shown in Fig. 3 are related to γ , β excitations and collective rotational modes described by Eq.(20). Since these low-lying excitations have been discussed

elsewhere [24], we will confine our study to the excitations at higher energy.

The moment $m_1(E2)$ exhausts more than 98% of the oscillator E2 energy-weighted sum rule (EWSR)

$$m_1(E2) = \frac{15}{2\pi} \frac{\hbar^2}{2m} A R_0^2$$

for all values of Ω . The same result holds for the $E0$ mode. Thus, the $E0$ and $E2$ EWSR are not affected by rotation.

The strength of the magnetic dipole transitions, at zero rotational frequency, is concentrated in three distinct regions, consistently with the theoretical expectations and the experimental findings [12]. We observe a low-energy interval ranging from 2 to 4 Mev, characterized by orbital excitations (scissors mode [10, 11]), a high-energy one around 24 MeV also arising from magnetic dipole orbital transitions (high energy scissors mode [38]), and a third intermediate region ranging from 4 to 12 MeV due to spin excitations [39].

As shown in Fig. 4, the distribution of the strength changes considerably as Ω increases, to the point that the dominant peak shifts from 7-8 MeV down to 3 MeV. Only at high

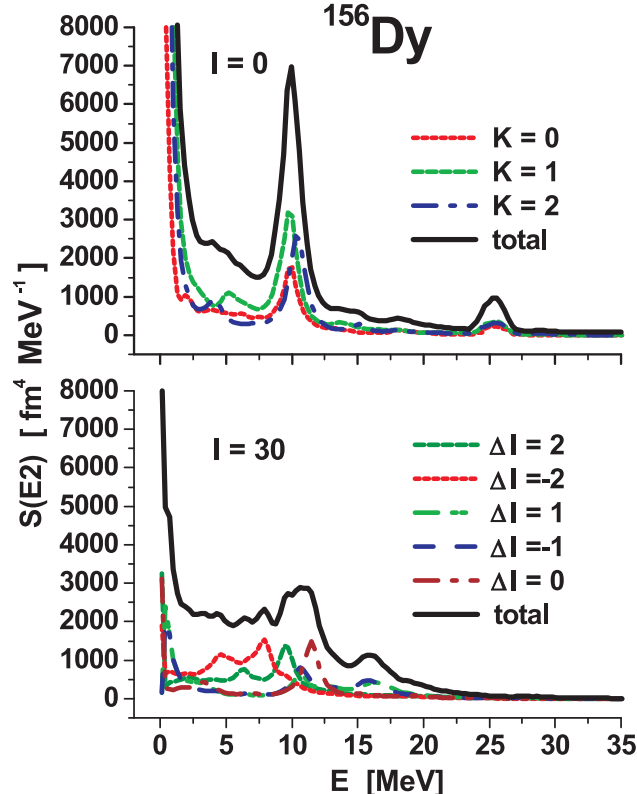


FIG. 3: (Color online) E2 strength function at zero and high rotational frequencies in ^{156}Dy .

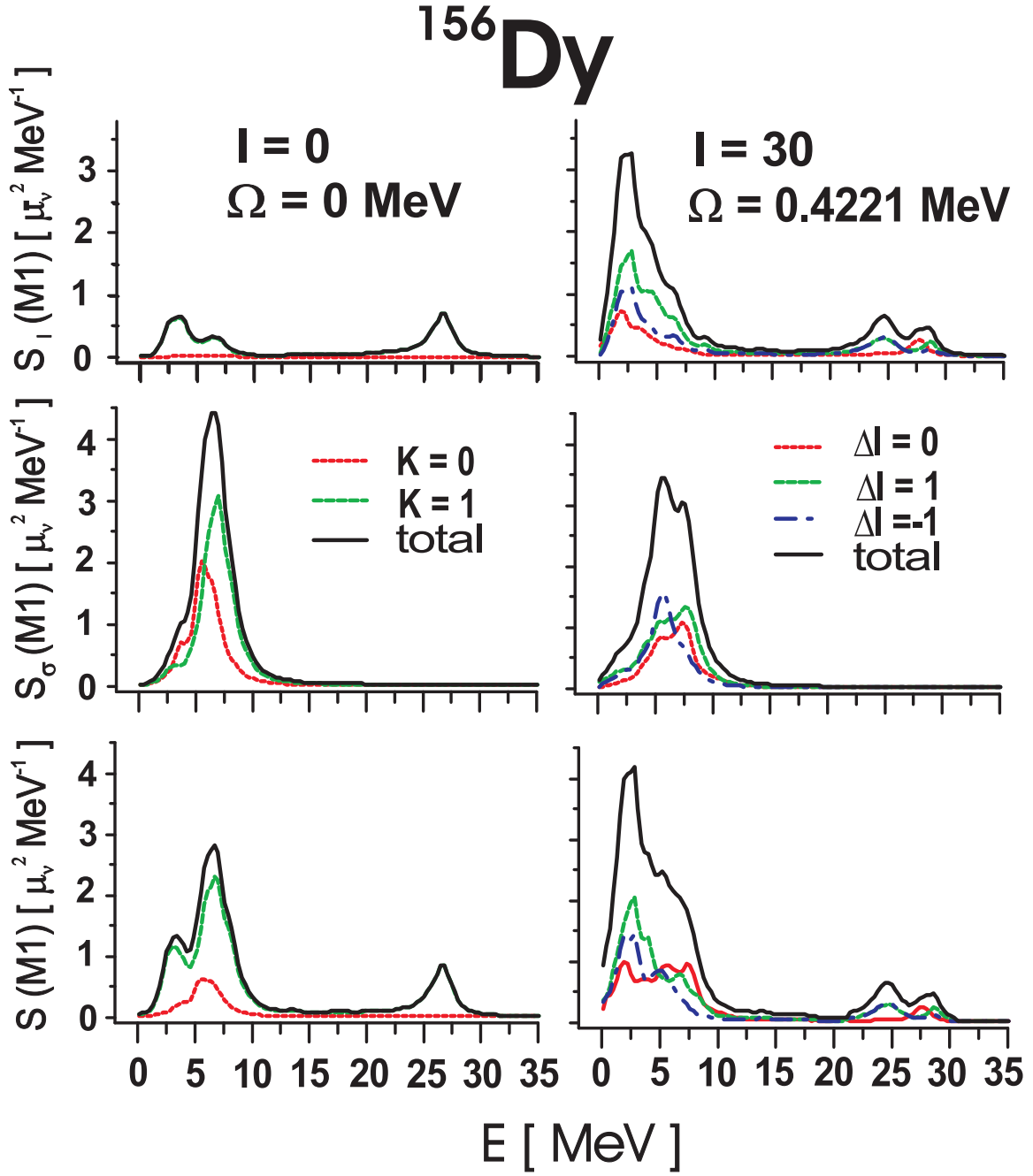


FIG. 4: (Color online) Orbital, spin, and total M1 strength functions at zero (left-hand panels) and high rotational frequencies (right-hand panels) in ^{156}Dy

energy, the changes are appreciable but not dramatic. In this region, in fact, the M1 strength gets more spread and increases slightly in magnitude (Table I).

In order to understand what is going on, we analyzed separately the contribution of the orbital and spin excitations up to 10 MeV. As shown in Fig. 5, the rotation broadens the spin

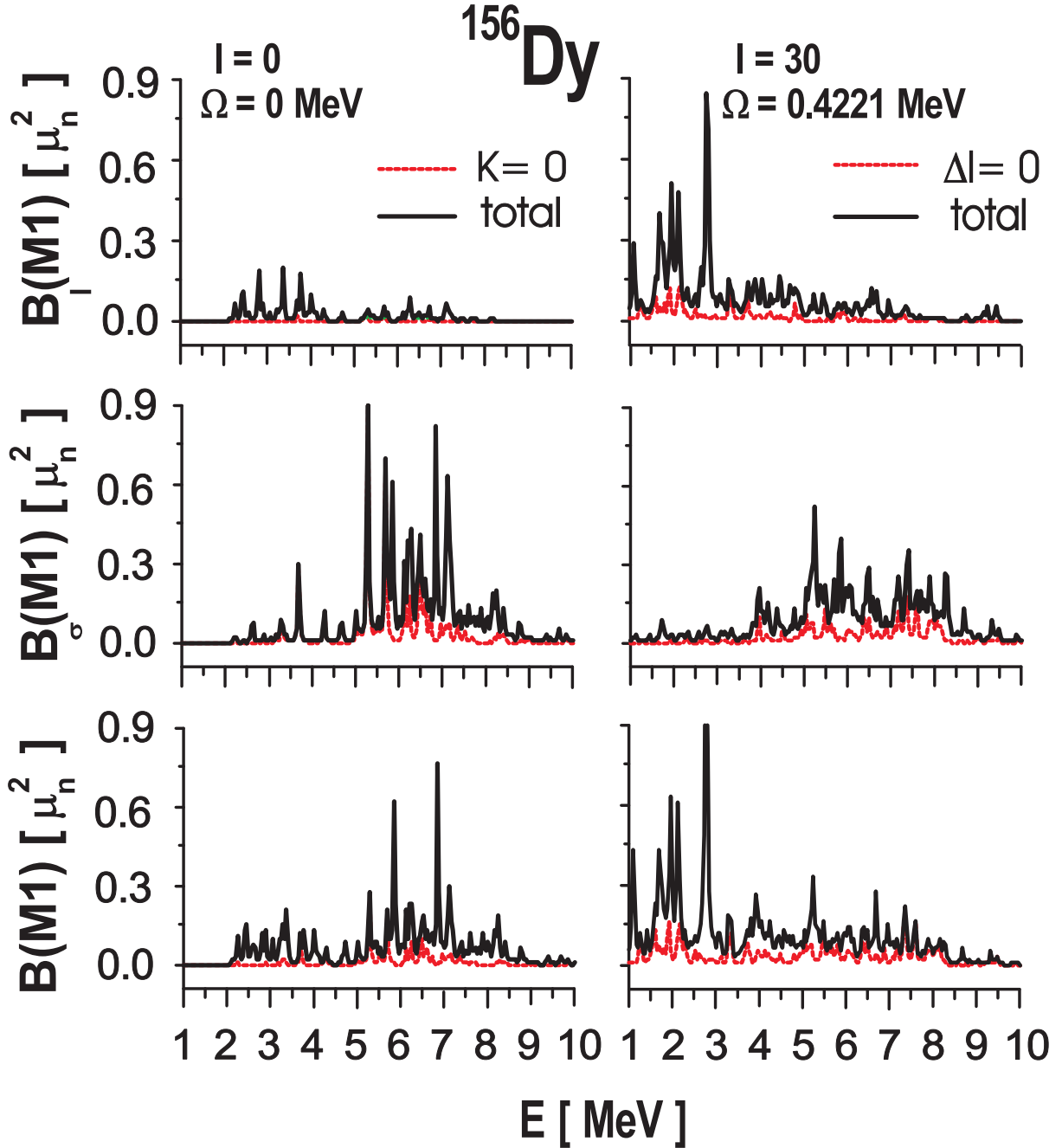


FIG. 5: (Color online) Orbital, spin, and total M1 reduced strength distributions at zero (left-hand panels) and high rotational frequencies (right-hand panels) in ^{156}Dy .

strength at the expenses of the main peaks which get severely reduced. The fragmentation keeps the spin transitions confined mainly within the range $4 \div 12$ MeV (Table I).

The low-lying orbital strength gets larger and larger with increasing Ω . At $\Omega = 0$, the orbital peaks are small compared to the spin transitions which dominate the M1 spectrum.

TABLE I: Orbital, spin and total M1 strengths integrated over different energy ranges at zero and high ($\Omega = 0.4221$ MeV) rotational frequencies.

	1MeV<E< 4MeV		4MeV<E< 12MeV		E > 12MeV	
	$I = 0$	$I = 30$	$I = 0$	$I = 30$	$I = 0$	$I = 30$
$\sum B_l(M1) [\mu_n^2]$	1.36	8.87	1.43	5.39	2.75	4.35
$\sum B_\sigma(M1) [\mu_n^2]$	1.92	3.08	14.97	14.47	0.48	0.68
$\sum B(M1) [\mu_n^2]$	2.95	12.21	9.82	10.06	3.57	4.58

At $I = 30\hbar$, instead, the orbital spectrum not only covers a wider energy range but gets magnified, specially in the low-energy sector, where quite high peaks appear. The low-lying orbital strength gets enhanced by more than a factor six because of the rotation (Table I). One may also observe that the $\Delta I = 0$ transitions, absent at zero frequency ($\Delta I = K = 0$), give a small but non zero contribution which increases with Ω . This is due to a new branch of the scissors mode which arises with the onset of triaxiality [40, 41]. Indeed, in going from axial to triaxial nuclei, the mode splits into two branches of energy and M1 strength

$$\begin{aligned} E_i &= \cos \gamma \left[1 - (-1)^i \frac{1}{\sqrt{3}} \tan \gamma \right] E_{sc}, \\ B_i(M1) &= \frac{1}{2} \cos \gamma \left[1 - (-1)^i \frac{1}{\sqrt{3}} \tan \gamma \right] B_{sc}(M1), \quad i = 1, 2 \end{aligned} \quad (31)$$

where E_{sc} and $B_{sc}(M1)$ are the energy and strength in the axial case. These two branches describe the rotational oscillations around the x_1 and x_2 axes. A new $K = 0$ branch also arises due to the rotational oscillation around the x_3 axis. Its energy and strength are given by

$$\begin{aligned} E_3 &= \frac{2}{\sqrt{3}} \sin \gamma E_{sc}, \\ B_3(M1) \uparrow &= \frac{2}{\sqrt{3}} \sin \gamma B_{sc}(M1). \end{aligned} \quad (32)$$

The increasing role of the orbital motion with increasing rotational frequency can be also inferred from the plot of the running sums shown in Fig. 6. The orbital strength, small at zero frequency in the whole energy range, at high frequencies becomes by far larger than the spin strength in the low-energy sector.

We can identify one of the mechanisms responsible for such a large enhancement by comparing (Fig. 7) the Ω dependence of the orbital and total $m_1(M1)$ moments with the

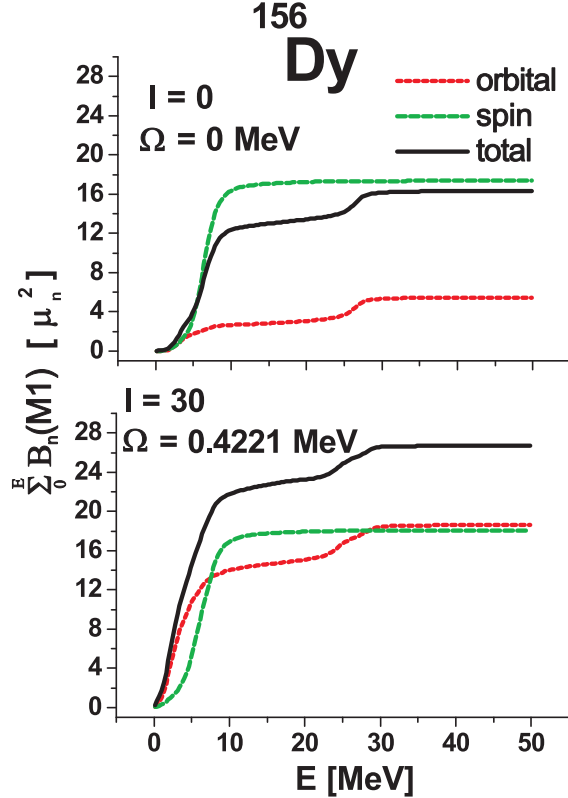


FIG. 6: (Color online) Running sum of the orbital (dashed line), spin (dashed-dot line) and total (solid line) M1 strength in ^{156}Dy .

corresponding evolution of the kinematical moment of inertia $\mathfrak{I} = I/\Omega$, computed using the cranking method of Ref. [30]. The strikingly similar behavior of the orbital $m_1(M1)$ and the moment of inertia shows that the two quantities are closely correlated at all rotational frequencies. Indeed, at zero frequency, one has the M1 EWSR [42, 43]

$$m_1^{(sc)}(M1) = \sum_n E_n B_n^{(sc)}(M1) \simeq \frac{9}{16\pi} (\kappa(0) - \kappa(1)) \langle Q(0) \rangle^2, \quad (33)$$

where $Q(0) = Q_p + Q_n$ is the isoscalar quadrupole field. Using the HO formulas (30) for the coupling constants and the standard expression for the quadrupole moment [1], we get for the right-hand side

$$m_1^{(sc)}(M1) = \frac{3}{8\pi} (1-b) \mathfrak{I}_{rig} \omega_0^2 \delta^2, \quad (34)$$

where $b = \kappa(1)/\kappa(0)$ and

$$\mathfrak{I}_{rig} = \frac{2}{3} m A \langle r^2 \rangle, \quad (35)$$

which shows explicitly the close link between the orbital M1 EWSR and the moment of inertia, at zero rotational frequency. We get a deeper insight by inspecting more closely

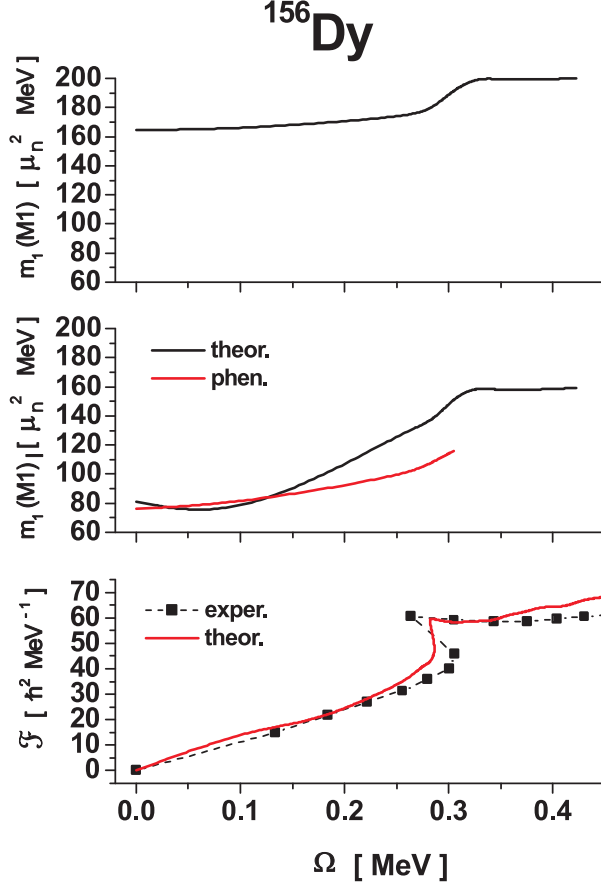


FIG. 7: (Color online) Total (top panel), orbital (middle panel) $m_1(M1)$ moments and the kinematical moment of inertia (bottom panel) versus Ω in ^{156}Dy . The dashed-dot line displays the M1 EWSR at zero frequency computed from Eq. (33) (taken from Ref. [43]).

the energy unweighted and weighted sums. For both low and high energy modes, the M1 summed strength has the general form [12]

$$m_0^{(\pm)}(M1) = \sum_{n_{\pm}} B_{n_{\pm}}^{(\pm)}(M1) \simeq \frac{3}{16\pi} \Im_{sc}^{(\pm)} \bar{E}^{(\pm)}, \quad (36)$$

having denoted by $\bar{E}^{(\pm)}$ and $\Im_{sc}^{(\pm)}$ the energy centroids and the mass parameters of the high-lying (+) and low-lying (-) scissors modes. At high energy, protons and neutrons behave as normal irrotational fluids, so that energy and mass parameter are given by

$$\bar{E}^{(+)} \propto 2\omega_0, \quad \Im_{sc}^{(+)} = \Im_{irr} = \Im_{rig} \delta^2, \quad (37)$$

yielding

$$m_0^{(+)}(M1) = \sum_{n_{+}} B_{n_{+}}^{(+)}(M1) \propto \Im_{rig} \delta^2$$

$$m_1^{(+)}(M1) \simeq \bar{E}^{(+)} \sum_{n_+} B_{n_+}^{(+)} \propto \Im_{rig} \delta^2. \quad (38)$$

Thus, both M1 weighted and unweighted summed strengths are quadratic in the deformation parameter. This result remains substantially unchanged in fast rotating nuclei.

For the low energy mode, instead, we must distinguish between zero and large rotational frequencies. At zero frequency, protons and neutrons behave as superfluids, so that [44, 45]

$$\bar{E}^{(-)} \propto 2E_{qp} \simeq 2\Delta, \quad \Im_{sc}^{(-)} = \Im_{sf} \propto \Im_{rig} \delta^2, \quad (39)$$

where E_{qp} denotes the quasiparticle energy and \Im_{sf} the superfluid moment of inertia. We then have

$$\begin{aligned} m_0^{(-)}(M1) &= \sum_{n_-} B_{n_-}^{(-)}(M1) \propto \Im_{rig} \delta^2 \\ m_1^{(-)}(M1) &\simeq \bar{E}^{(-)} \sum_{n_-} B_{n_-}^{(-)}(M1) \propto \Im_{rig} \delta^2. \end{aligned} \quad (40)$$

These relations show that $m_1(M1)$ is consistent with the EWSR (33) and, quite remarkably, the summed strength $m_0(M1)$ follows the quadratic deformation law found experimentally [46, 47].

At high rotational frequency, instead, the pairing correlations are quenched, so that protons and neutrons behave basically as rigid rotors. We have therefore

$$\bar{E}^{(-)} \propto \delta\omega_0, \quad \Im_{sc}^{(-)} \simeq \Im_{rig}, \quad (41)$$

which yield

$$\begin{aligned} m_0^{(-)}(M1) &= \sum_{n_-} B_{n_-}^{(-)} \propto \Im_{rig} \delta \\ m_1^{(-)}(M1) &\simeq \bar{E}^{(-)} \sum_{n_-} B_{n_-}^{(-)} \propto \Im_{rig} \delta^2. \end{aligned} \quad (42)$$

According to the above formulas, the superfluid to normal phase transition affects the deformation law. While, in fact, the energy-weighted sum remains quadratic in the deformation, the behavior of the unweighted summed strength with δ changes from quadratic to linear.

We can therefore conclude that the scissors M1 strength is closely correlated with the nuclear moment of inertia not only at low but also at large rotational frequency. More in detail, while the quasiparticle energy moves downward because of the weakening of pairing, the $M1$ strength increases with Ω before backbending because of the increasing axial deformation and the gradual enhancement of the moment of inertia. Above the backbending

critical value, when the nucleus undergoes a transition from a superfluid to an almost rigid phase, as result of the the alignment of few quasiparticles with high spin, the $M1$ strength jumps to a plateau, due to a sudden increase of the moment of inertia, while the deformation parameter δ remains practically constant.

Also the onset of triaxiality raises $m_1(M1)$ at large rotational frequency, to a modest extent. Indeed, from Eqs. (31) and (32) we get ($i = 1, 2, 3$)

$$\sum_i E_i^{(-)} B_i^{(-)}(M1) \uparrow= \left(1 + \frac{5}{18} \sin^2 \gamma\right) m_1^{(-)}(M1) \quad (43)$$

For $\gamma = 50^0$ the $m_1^{(-)}(M1)$ gets enhanced by a factor 1.16. A further contribution comes from the changes in the shell structure induced by the rotation which increase the number of configurations taking part to the motion over the whole energy range. The new configurations generate new transitions on one hand, and, on the other hand, enhance the amplitudes of collective as well non collective transitions.

IV. CONCLUSIONS

Our analysis shows that fast rotation strengthens the coupling between quadrupole and monopole modes, broadens appreciably the isoscalar quadrupole giant resonance and washes out the isovector monopole and quadrupole peaks. These rotation induced effects are found to be more appreciable than what predicted in Ref. [23]. On the other hand, the two approaches differ in several details. We accounted for the $\Delta N = 2$ coupling in generating the Nilsson states and included the Galilean invariance restoring piece according to the prescription of Ref. [18]. Moreover, we enforced the HB stability conditions, provided by Eq.(10), that yield deformation parameters very close to the self-consistent values and fixed the strength parameters of the interaction so as to guarantee the separation of the spurious modes from the intrinsic excitations at each rotational frequency.

The most meaningful and intriguing result of our calculation concerns the orbital, scissors-like, $M1$ excitations. The enhancement of the overall $M1$ strength at high rotational frequencies emphasizes the dominant role of the scissors mode over spin excitations in fast rotating nuclei and represents an additional signature for superfluid to normal phase transitions in deformed nuclei. If confirmed experimentally, this feature would provide new information on the collective properties of deformed nuclei.

Acknowledgments

This work was partly supported by the Czech grant agency under the contract No. 202/02/0939, the Italian Ministero dell'Istruzione, Università and Ricerca (MIUR) and by the Grant No. BFM2002-03241 from DGI (Spain). R. G. N. gratefully acknowledges support from the Ramón y Cajal program (Spain).

- [1] A. Bohr and B.R. Mottelson, *Nuclear Structure* (Benjamin, New York, 1975) Vol.II.
- [2] M. Danos, Nucl. Phys. **5**, 23 (1958).
- [3] K. Okamoto, Phys. Rev. **110**, 143 (1958).
- [4] T. Kishimoto, J. M. Moss, D.H. Youngblood, J.D. Bronson, C.M. Rozsa, D.R. Brown, and A.D. Bacher, Phys. Rev. Lett. **35**, 552 (1975).
- [5] T. Nakatsukasa, K. Matsuyanagi, and S. Mizutori, Prog. Theor. Phys **87**, 607 (1992).
- [6] R. Nazmitdinov and S. Åberg, Phys. Lett. B **289**, 238 (1992).
- [7] T. Suzuki and D.J. Rowe, Nucl. Phys. A **289**, 461 (1978).
- [8] D. Zawischa, J. Speth, and D. Pal, Nucl. Phys. A **311**, 445 (1978).
- [9] S. Aberg, Nucl. Phys. A **473**, 1 (1987).
- [10] N. Lo Iudice and F. Palumbo, Phys. Rev. Lett. **41**, 1532 (1978).
- [11] D. Bohle, A. Richter, W. Steffen, A.E.L. Dieperink, N. Lo Iudice, F. Palumbo, and O. Scholten, Phys. Lett. B **137**, 27 (1984).
- [12] For an exhaustive list of reference N. Lo Iudice, Rivista Nuovo Cimento **9**, 1 (2000).
- [13] P. Ring and P. Schuck, *The Nuclear Many-Body Problem* (Springer-Verlag, New York, 1980) for references.
- [14] J. Kvasil and R.G. Nazmitdinov, Fiz. Elem. Chastits At. Yadra **17**, 613 (1986) [Sov. J. Part. Nucl. **17**, 265 (1986)].
- [15] Y.R. Shimizu and M. Matsuzaki, Nucl. Phys. A **558**, 559 (1995).
- [16] L.M. Robledo, J.L. Egido, and P. Ring, Nucl. Phys. A **449**, 201 (1986).
- [17] R.G. Nazmitdinov, Yad. Fiz. **46**, 732 (1987) [Sov. J. Nucl. Phys. **46**, 412 (1987)].
- [18] T. Nakatsukasa, K. Matsuyanagi, S. Mizutori, and Y.R. Shimizu, Phys. Rev. C **53**, 2213 (1996).

- [19] Y.R. Shimizu, J.D. Garrett, R.A. Broglia, M. Gallardo, and E. Vigezzi, Rev. Mod. Phys. **61**, 131 (1989).
- [20] D. Almehed D, F. Dönau, S. Frauendorf, and R.G. Nazmitdinov, Phys.Scr. **T88** 62 (2000); D. Almehed, S. Frauendorf, and F. Dönau, Phys. Rev. C **63** 044311 (2001).
- [21] K. A. Snover, Ann. Rev. Nucl. Part. Sci. **36**, 545 (1986) and references therein.
- [22] J.J. Gaardhøje, Ann. Rev. Nucl. Part. Sci. **42**, 483 (1992) and references therein.
- [23] Y.R. Shimizu and K. Matsuyanagi, Progr. Theor. Phys. **72**, 1017 (1984); *ibid* **75**, 1167 (1986).
- [24] see for instance J. Kvasil and R.G. Nazmitdinov, preprint nucl-th/0402031, to be published in Phys. Rev. C ; J. Kvasil, R.G. Nazmitdinov, and A.S. Sitzdikov, to be published in Yadernaya Fizika .
- [25] C. De Coster and K. Heyde, Phys. Rev. Lett. **63**, 2797 (1989).
- [26] C. De Coster and K. Heyde, Nucl. Phys. **A 524**, 441 (1991).
- [27] J. Kvasil, N. Lo Iudice, V.O. Nesterenko, and M. Kopal, Phys. Rev. C **58**, 209 (1998).
- [28] H. Sakamoto and T. Kishimoto, Nucl. Phys. A **501**, 205 (1989).
- [29] N. Lo Iudice, Nucl.Phys. **A 605**, 61 (1996).
- [30] D. Almehed, F. Dönau, and R.G. Nazmitdinov, J. Phys. G: Nucl. Part. Phys. **29**, 2193 (2003).
- [31] R.G. Nazmitdinov, D. Almehed, and F. Dönau, Phys. Rev. C **65**, 041307(R) (2002).
- [32] E.R. Marshalek, Nucl. Phys. A **266**, 317 (1976).
- [33] A.K. Jain, R.K. Sheline, P.C. Sood, and K. Jain, Rev. Mod. Phys. **62**, 393 (1990).
- [34] R. Wyss, W. Satula, W. Nazarewicz, and A. Johnson, Nucl. Phys. A **511**, 324 (1990).
- [35] R.Ch. Safarov and A.S. Sitzdikov, Izv. A.N. **63**, 162 (1999) and references therein.
- [36] S. Frauendorf and F.R. May, Phys. Lett. B **125**, 245 (1983).
- [37] B. Castel and I. Hamamoto, Phys. Lett B **65**, 27 (1976).
- [38] N. Lo Iudice and A. Richter Phys. Lett. B **228**, 291 (1989).
- [39] A. Richter, Nucl. Phys. A **553**, 417c (1993)
- [40] F. Palumbo and A. Richter, Phys. Lett. B **158**, 101 (1985).
- [41] N. Lo Iudice, E. Lipparini, S. Stringari, F. Palumbo, and A. Richter, Phys. Lett. B **161**, 18 (1985).
- [42] L. Zamick and D.C. Zheng, Phys. Rev. C **44**, 2522 (1991).
- [43] N. Lo Iudice, Phys. Rev. C **57**, 1246 (1998).
- [44] N. Lo Iudice and A. Richter Phys. Lett. B **304**, 193 (1993).

- [45] N. Pietralla, P. von Brentano, R.-D. Herzberg, U. Kneissl, N. Lo Iudice, H. Maser, H. H. Pitz, and A. Zilges, Phys. Rev. C **58**, 184 (1998).
- [46] W. Ziegler, C. Rangacharyulu, A. Richter, and C. Spieler, Phys. Rev. Lett. **65**, 2515 (1990).
- [47] J. Margraf, R.D. Heil, U. Kneissl, U. Meier, H.H. Pitz, H. Friedrichs, S. Lindenstruth, B. Schlitt, C. Wesselborg, P. von Brentano, R.-D. Herzberg, and A. Zilges, Phys. Rev. C **47**, 1474 (1993).